Journal of Applied Polymer Science

Effect of molecular rigidity and hydrogen bond interaction on mechanical properties of polyimide fibers

Yan Feng, Long Bo Luo, Jieyang Huang, Ke Li, Baoying Li, Huina Wang, Xiangyang Liu
State Key Laboratory of Polymer Material and Engineering, College of Polymer Science and Engineering, Sichuan University, Chengdu 610065, People's Republic of China
Correspondence to: X. Liu (E-mail: lxy6912@sina.com)

ABSTRACT: Six kinds of polyimide (PI) fibers with different molecular rigidity and hydrogen bond interactions were designed and prepared in order to investigate the relationship between structure and mechanical properties. The rigidity, aggregation structure, fracture morphology, hydrogen bond, and charge transfer (CT) interactions were investigated in detail. Conformational rigidity of six PI fibers were simulated and measured by *D*-values of energy barrier and bottom in potential energy curves of PI units. Rigid rod-like PI macromolecules tend to pack in order and show better mechanical properties. However, with the increase of *D*-values, fracture mechanisms change from ductile fracture to brittle fracture. Brittle fracture resulting from high conformational rigidity is adverse to improvement of mechanical properties of PI fibers. Besides, strength of hydrogen bond and CT interactions are characterized by infrared spectroscopy and ultraviolet absorption spectra, respectively. The results indicate that higher interactions lead to higher tensile strength and initial modulus. Finally, PI fibers, which possess moderate conformational rigidity and strong hydrogen bond interactions, exhibit highest tensile strength (1.82 GPa) and initial modulus (85.7 GPa) in six kinds of PI fibers. © 2016 Wiley Periodicals, Inc. J. Appl. Polym. Sci. **2016**, *133*, 43677.

KEYWORDS: crystallization; mechanical properties; polyimides; properties and characterization

Received 3 November 2015; accepted 22 March 2016
DOI: 10.1002/app.43677

INTRODUCTION

Polyimide (PI) fibers play a critical role in high-performance fibers production since 1960s due to their excellent thermal stability, chemical resistance, filter efficiency, radiation resistance, and low dielectric constant.[1] These advantages of PI fibers are attributed to high bond energy, strong intermolecular interactions, and conjugated effect of PI molecules, which leads to potential application of PI fibers in filter, fire-proofing, microelectronics, atomic energy, and astronautics industry.[2] Compared with other high-performance fibers, PI fibers are mainly used as high temperature filter material. Tensile strength of 0.5 GPa is enough for PI fibers in this area. However, many researchers hope to use PI fibers in advanced composite materials due to their excellent radiation resistance and high thermal properties.[3–6] Tensile strength of fibers used in advanced composite materials should be above 2.5 GPa at least. For example, tensile strength of Kevlar is about 2.9 GPa. However, it is difficult for PI fibers.[7,8] For instance, Park and Farris had prepared pyromellitic dianhydride/4,4′-oxydianiline (PMDA/ODA) PI fibers with the tensile strength of 0.399 GPa and initial modulus of 5.2 GPa.[9] In addition, as commercial PI fibers, the tensile strength of P84, whose application majored in thermal filter field, was only 0.53 GPa.[9] Thus, as high performance fibers, the mechanical properties of PI fibers need to be highly enhanced.

To improve the mechanical properties of PI fibers, molecular design of PI molecule has been focused in the past decades. Many researchers have demonstrated that PI fibers with more rigid backbones lead to more excellent mechanical properties. As an alternative approach, benzimidazole units are introduced into the PI main chain by many researchers in recent years.[4–6,8,10–23] For example, in our previous work, a series of copolyimide (co-PI) fibers containing benzimidazole moieties in the PI main chains were prepared. When the diamine ratio of 2-(4-aminophenyl)-5-aminobenzimidazole were 70%, the tensile strength reached 1.53 GPa, which were almost three times over PMDA/ODA PI fibers.[10,11] Yin *et al.* prepared a series of rigid-rod co-polyimide (co-PI) fibers containing benzimidazole and benzoxazole moieties with 2-(4-aminophenyl)-5-aminobenzimidazole (BIA), 5-amino-2-(4-aminobenzene) benzoxazole (BOA), and BPDA. The optimum tensile strength and modulus of co-PI

Additional Supporting Information may be found in the online version of this article.

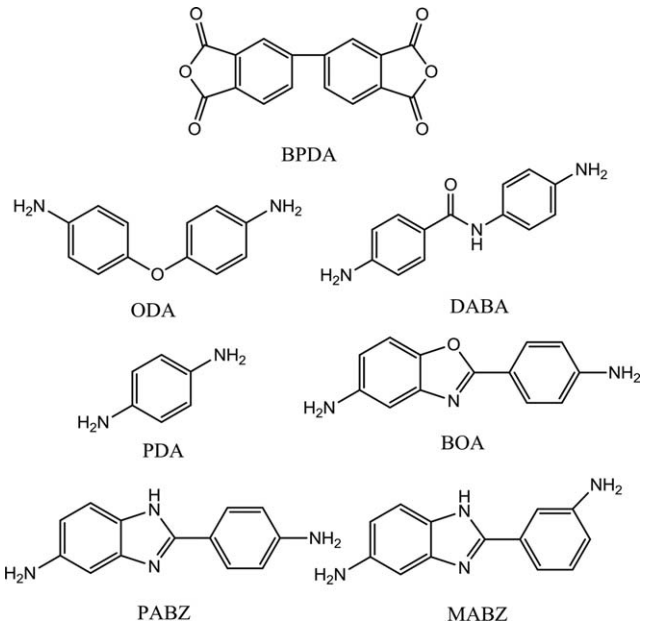

Scheme 1. The structures of one dianhydride and six kinds of diamides.

fibers are as high as 1.74 and 74.4 GPa at the BIA/BOA molar ratio of 7/3.[17] Dong *et al.* prepared a type of PI fiber based on 2,2′-bis(trifluoromethyl)-4,4′-diaminobiphenyl (TFMB), 2-(4-aminophenyl)-5-aminobenzimidazole (BIA) and BPDA, showing a tensile strength of 2.15 GPa with a modulus of 105 GPa.[4] Consequently, PI fibers containing benzimidazole units have the potential to become representative of PI fibers with high strength and modulus for enhancement of intermolecular interactions.[24]

As we know, except for intermolecular interactions, conformational rigidity is the most important factor for high performance polymer fibers. Poly[(benzo1,2-d:5,4-d′bisoxazole-2,6-diyl)-1,4-phenylene] (PBO) is one of typical rigid-rod ordered polymers, whose tensile strength and modulus are as high as 5.6 GPa and 352 GPa, respectively.[24] However, there is no systematic study on the effect of intermolecular interactions and rigidity on the aggregation structure and mechanical properties of PI fibers.

In this study, six kinds of homo PIs with different molecular rigidity and hydrogen bond interactions were designed and prepared by wet spinning method. Rigidity of molecule was measured by *D*-values of energy barrier and bottom in potential energy curves of PI units. The relationships of mechanical properties with rigidity, intermolecular interactions, and aggregation structure of PI fibers were investigated. It was found that PI fibers, which possess moderate conformational rigidity and strong hydrogen bond interactions, exhibit highest tensile strength and initial modulus in six kinds of PI fibers.

EXPERIMENTAL

Materials

N-Methyl-2-pyrrolidone (NMP) was obtained from Puyang MYJ Technology Co., Ltd., China. and was distilled under reduced pressure before use. 4,4-Oxydianiline (ODA) was obtained from Changshou Chemical Company, China. 4-Amino-*N*-(4-aminophenyl) benzamide (DABA), *p*-phenylenediamine (PDA), 2-(4-aminophenyl)-5(6)-aminobenzoxazole (BOA), 2-(4-aminophenyl)-5(6)-aminobenzimidazole (PABZ), 2-(3-aminophenyl)-5(6)-aminobenzimidazole (MABZ), and 3,3′,4,4′-biphenyltetracarboxylic dianhydride (BPDA) were obtained from Changzhou Sunlight Medical Raw Material Co., Ltd., China. BPDA was dried at 200 °C in an oven for 10 h. The structures of the monomers are shown in Scheme 1.

Synthesis of Polyamide Acid

Polyamide acid (PAA) solutions were prepared by stirring equimolar amounts of dianhydride and diamine in NMP under a nitrogen atmosphere at room temperature for 50 h. The solid contents of BPDA/ODA, BPDA/PDA, BPDA/DABA, BPDA/BOA, BPDA/PABZ, and BPDA/MABZ PAA solutions were 10%, 10%, 10%, 12%, 12%, and 12%, respectively.

Preparation of PAA and PI Fibers

The PAA solutions were filtered and degassed at reduced pressure for 24 h prior to use. PAA fibers were prepared by wet-spinning. Detailed spinning routes have been described previously.[8] In the second stage, the PI fibers were obtained by thermal imidization of PAA fibers without tension during the heating at 6–8 °C/min to 420 °C for 10 min. Scheme 2 shows the synthetic process and the chemical structure of the PIs.

Characterization

Mechanical properties of PAA and PI fibers were tested on YG001A-1 Fiber Electronic Strength Tester with a strain rate of 5 mm/min. The fixture span of fiber tests was set as 20 mm. The intrinsic viscosity of PAA solution was measured with an ubbelohde viscometer in 0.5 dL/g NMP at 30 °C. One-dimensional Wide angel X-ray diffraction (1D-WAXD) patterns of PI fibers were measured with a Philips X'Pert PRO MPD. X-ray diffraction measurements were taken from reflection mode at room temperature, using Ni-filtered Cu Kα radiation operated at 40 kV × 40 mA. Two-dimensional wide angel X-ray diffraction (2D-WAXD) patterns of the fibers were collected on a Bruker D8 Discover with VÅNTEC-500 detectors with patented Mikrogap. Attenuated total reflection infrared spectroscopy-Fourier transform infrared (ATR-FTIR) spectra of PI fibers were measured at a Nicolet Magna 650 spectroscope in the range 4000–400 cm^{-1}. The frequency scale was internally calibrated with a reference helium–neon laser to an accuracy of 0.2 cm^{-1}. Fractured morphologies of the fibers were observed on a JEOL JSM-5900LV scanning electron microscope (SEM). Dynamic mechanical analysis

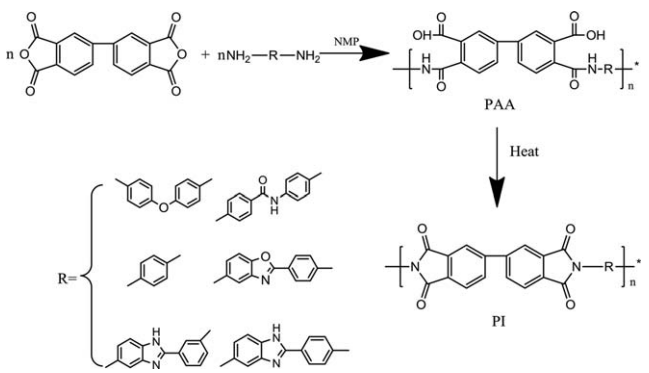

Scheme 2. The synthetic process and the chemical structure of the PIs.

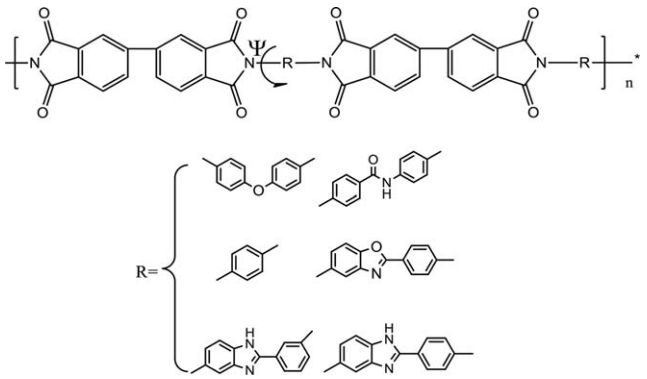

Scheme 3. The dihedral angle Ψ rotated in six kinds of PI unit.

(DMA) was carried out on a TA Q800 instrument under N_2 atmosphere with a heating rate of 10°C/min from 40 to 550°C, and the load frequency was 1 Hz. UV/vis transmission spectroscopy was measured at a UV-1800PC Spectrophotometer in the range 200–800 nm. Potential energy curve of torsion was calculated by molecular dynamics simulation with Materials Studio 4.0 software to measure the rigidity of PI repeat unit. The dihedral angle Ψ selected to be simulated is shown in Scheme 3. Highest occupied molecular orbital (HOMO) energy level and lowest unoccupied molecular orbital (LUMO) energy level were calculated with Gaussian 03 base on density functional theory (DFT).

RESULTS AND DISCUSSION

Chemical Structure

The ATR-FTIR results of six kinds of PI fibers are shown in Figure 1. All the PI fibers exhibit characteristic peaks at around 1380 cm^{-1} (the stretching of C—N vs C—N), 1720 cm^{-1} (the asymmetric stretching of the imide carbonyls vs C═O) and 1780 cm^{-1} (the symmetric stretching of the imide carbonyls vs C═O), respectively.[15] The absence of peaks near 1650 and 1550 cm^{-1} indicates that polyamic acid has disappeared after curing.[13] These results indicate that PI fibers were successfully prepared. Besides, in ATR-FTIR spectrum of BPDA/ODA PI fibers, stretching vibration peak of —O— is observed at 1240 cm^{-1}.[25] In ATR-FTIR spectrum of BPDA/DABA PI fibers, stretching vibration absorption of amide carbonyl locates at 1660 cm^{-1}, indicating the existence of amide bonds.[12] In ATR-FTIR spectrum of BPDA/BOA PI fibers, peaks at 1560 cm^{-1} and 1480 cm^{-1} wavenumber correspond to stretching vibration peak of benzoxazole, and the peak at 925 cm^{-1} wavenumber is attributed to bending vibration absorption of O—C═N.[26] In ATR-FTIR spectra of BPDA/PABZ and BPDA/MABZ PI fibers, characteristic peaks at 1478 cm^{-1} and 1450 cm^{-1} wavenumber confirm the structure of benzimidazole.[26] In ATR-FTIR spectra of BPDA/DABA, BPDA/MABZ, and BPDA/PABZ PI fibers, a broad peak ranging from 3000 cm^{-1} to 3500 cm^{-1} is observed, indicating the formation of hydrogen bond interactions derived from N—H of amide bond and benzimidazole.[3] Peak of —NH— shifts toward lower wavenumber with enhancement of strength of hydrogen bond interactions. Compared with BPDA/DABA, peak of —NH— in spectrum of BPDA/PABZ shifts 26 cm^{-1} wavenumber, from 3369 cm^{-1} to 3343 cm^{-1}. Compared with BPDA/PABZ, peak of —NH— in spectrum of BPDA/MABZ shifts 6 cm^{-1} wavenumber, from 3343 cm^{-1} to 3337 cm^{-1}. So the order of strength of hydrogen bond interactions is BPDA/DABA < BPDA/PABZ < BPDA/MABZ.

Intrinsic Viscosity and Mechanical Properties of PAA Fibers

Generally, mechanical properties of PI fibers are influenced by intrinsic viscosity, physical defect, imidization degree, rigidity of molecular chains, interactions between molecular chains, and aggregation structure.

Gel permeation chromatography (GPC) is a direct method to determine the molecular weight of PAA,[27,28] while the intrinsic viscosity of polyamic acid is a simple and effective method to characterize the molecular weight indirectly. In this article, we choose intrinsic viscosity of polyamic acid to compare the molecular weight. The intrinsic viscosities of six different PAA fibers are shown in Supporting Information Table S1. The intrinsic viscosities of BPDA/PDA, BPDA/BOA, and BPDA/PABZ PAA solution are 2.4 dL/g–2.6 dL/g, lower than that of BPDA/ODA, BPDA/DABA, and BPDA/MABZ PAA solution. Moreover, the tensile strength of six PAA fibers is nearly the same, as shown in Supporting Information Table s1. Those results indicate that molecular weight and techniques of spinning should make little contribution to the difference in mechanical properties.

The Fracture Morphologies

The fracture morphologies of six PI fibers were studied by SEM, as shown in Figure 2. The cross-sections of six kinds of PI fibers are round and voids-free, indicating that there is no obvious physical defect harming the mechanical properties of PI fibers.

As the imidization degrees of six kinds of PI fibers can be calculated to be above 98% from the ATR-FTIR results, imidization degree makes no contribution to the difference in mechanical properties. In summary, the difference in mechanical properties is not caused by intrinsic viscosity, physical defect, or imidization degree. For the aggregation structure is also affected by rigidity of molecular chains and interactions between molecular chains, the difference in mechanical properties is brought by distinction in rigidity of molecular chains and interactions between molecular chains.

Macromolecular Chain Rigidity

Among six kinds of PI fibers, the main chain of BPDA/ODA is a flexible molecular chain. BPDA/DABA contains amide bond, so that there are strong interactions between molecular chains. The main chain of BPDA/PDA is a typical rigid-rod molecular chain. The main chains of BPDA/BOA and BPDA/PABZ are both rigid molecular chains and the difference is that there are strong interactions between BPDA/PABZ molecular chains brought by imidazole. The main chain of MABZ/BPDA is a flexible molecular chain with strong interactions for its meta-position structure.

Potential energy curves of torsion of six PI units at 300 K were simulated with Materials Studio 4.0 software. *D*-value of energy barrier and bottom in potential energy curve is calculated to measure the conformational rigidity,[29,30] as shown in Figure 3. The larger the *D*-value is, the more energy molecular chains needed when rotating from one potential bottom to another.

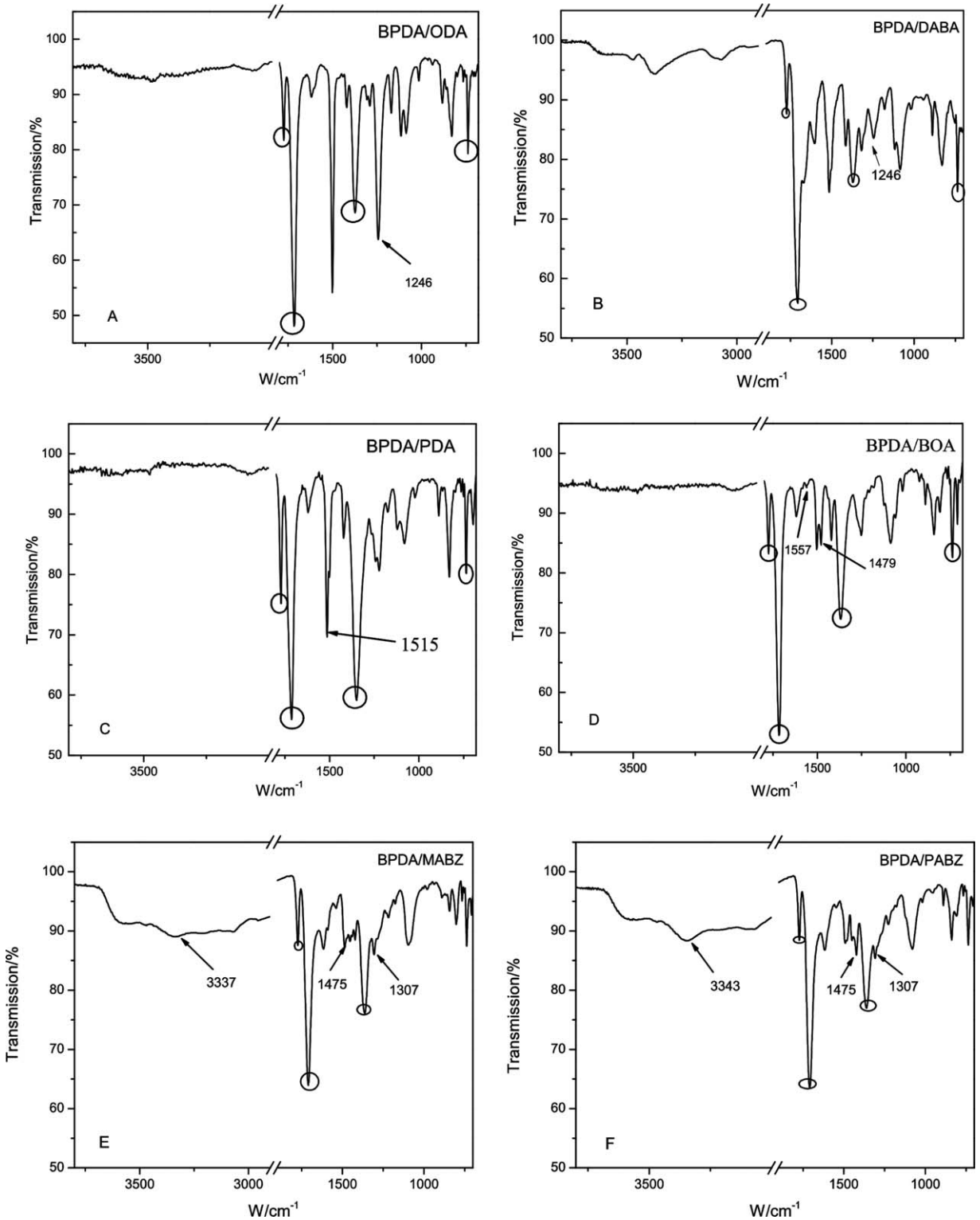

Figure 1. ATR-FTIR spectra of (A) BPDA/ODA; (B) BPDA/DABA; (C) BPDA/PDA; (D) BPDA/BOA; (E) BPDA/MABZ; (F) BPDA/PABZ PI fibers.

The more difficultly molecular chains rotate, the more rigid the molecular chains are. *D*-values of energy barrier and bottom can be clearly seen in Figure 3. Therefore the order of rigidity of six PI fibers is BPDA/PDA > BPDA/PABZ > BPDA/BOA > BPDA/DABA > BPDA/ODA > BPDA/MABZ.

Glass-Transition Temperature

DMA curves are shown in Figure 4. The glass-transition temperature (T_g) values are regarded as the peak temperature in the internal loss factor (tan δ) curves.[18–23] For BPDA/ODA, BPDA/BOA, BPDA/PDA, BPDA/DABA, BPDA/PABZ, and BPDA/MABZ PI

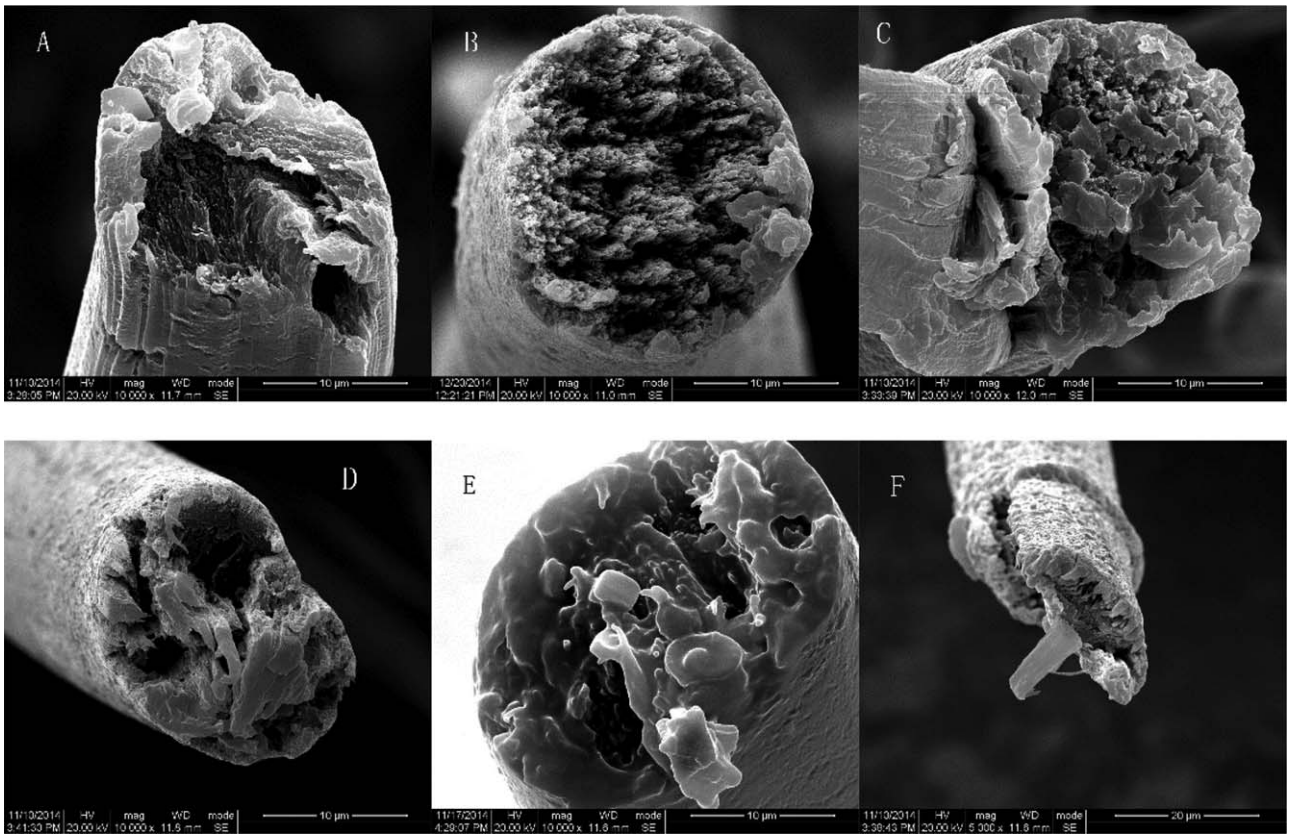

Figure 2. Fracture morphology of (A) BPDA/ODA; (B) BPDA/DABA; (C) BPDA/PDA; (D) BPDA/MABZ; (E) BPDA/BOA; (F)BPDA/PABZ PI fibers.

fibers, T_gs are 284, 292, 325, 335, 370, and 408 °C In classical polymer physics, high T_g represents high rigidity and strong chain–chain interactions.[31] The increasing T_g values of BPDA/ODA, BPDA/BOA, and BPDA/PDA PI fibers confirm the order of rigidity in molecular simulations. In BPDA/PABZ PI molecules, —NH— replaces the position of benzoxazole —O— in BPDA/BOA

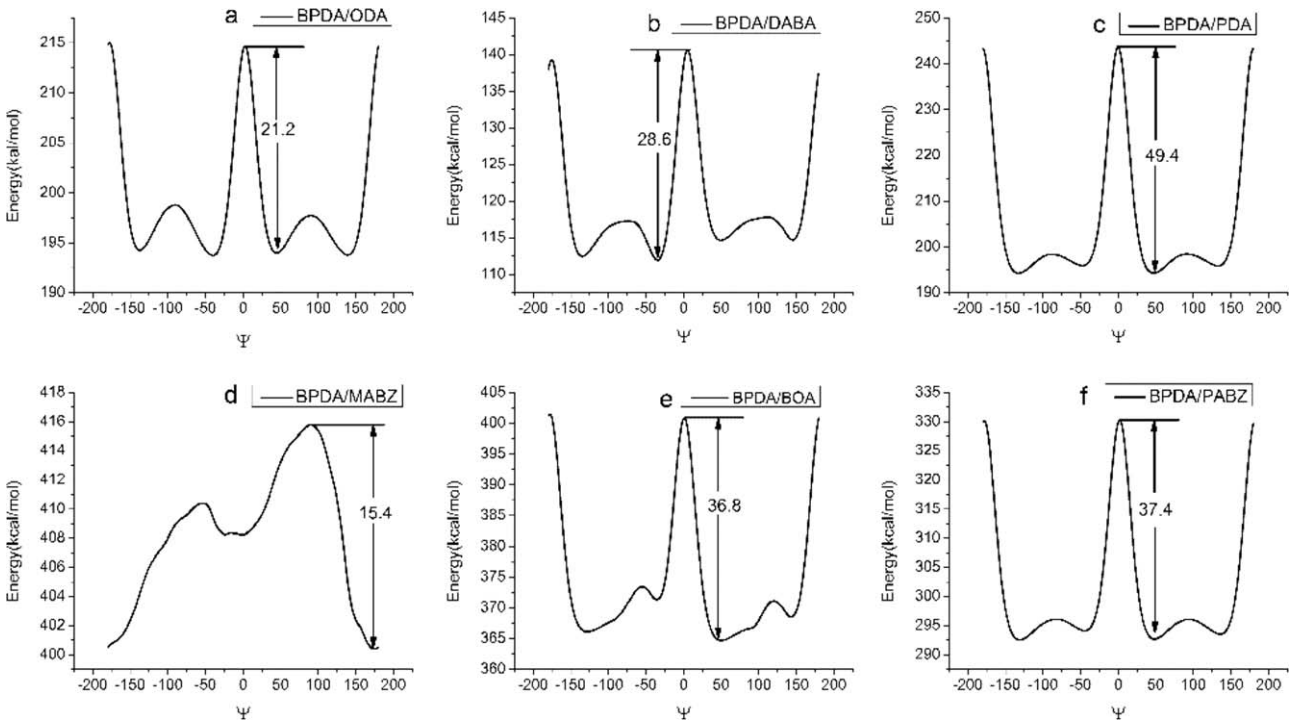

Figure 3. Potential energy curves of Ψ in (a) BPDA/ODA; (b) BPDA/DABA; (c) BPDA/PDA; (d) BPDA/MABZ; (e) BPDA/BOA; (f) BPDA/PABZ PI units.

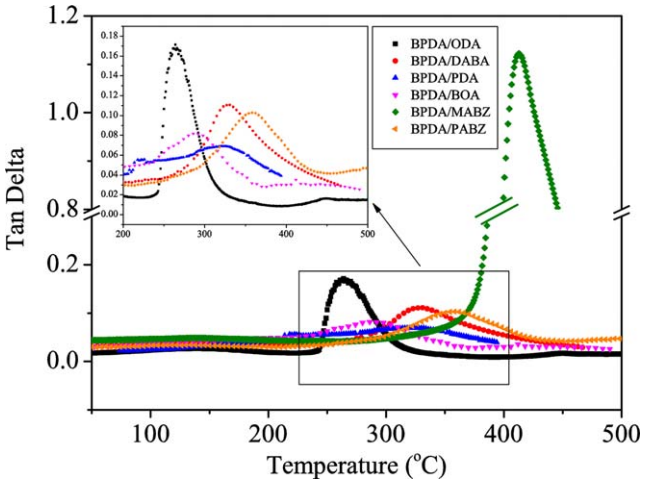

Figure 4. The DMA curves of six kinds of PI fibers. [Color figure can be viewed in the online issue, which is available at wileyonlinelibrary.com.]

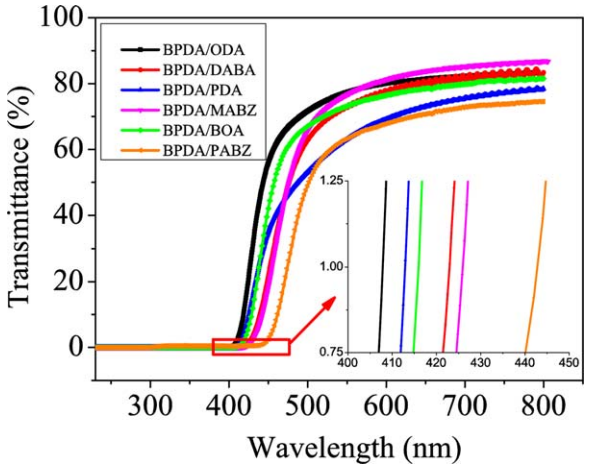

Figure 5. The UV/vis transmission spectra of six kinds of PI films after annealing at 380 °C. [Color figure can be viewed in the online issue, which is available at wileyonlinelibrary.com.]

systems, and the results of molecular simulations also show that the two systems share similar rigidity. Therefore, the T_g gap of 78 °C indicates strong hydrogen bond interactions brought by —NH—. Similarly, T_g of BPDA/DABA fibers is 51 °C higher than BPDA/ODA fibers, as a result of strong hydrogen bond interactions brought by amide bond. Besides, the flexible BPDA/MABZ PI fibers show highest T_g, reflecting that hydrogen bond interactions between molecular chains are the strongest. These results are in accordance with the order of strength of hydrogen bond proved by ATR-FTIR well. Moreover, as we know, the intensity of the tan δ at T_g is an evaluation of the energy-damping characteristic of a material, which is influenced by rigidity and crystallinity. As indicated in Figure 4, the tan δ values of flexible PI fibers (BPDA/MABZ, BPDA/MABZ, and BPDA/DABA) are larger than rigid PI fibers (BPDA/PABZ, BPDA/BOA, and BPDA/PDA). This also suggests a hindered rotation of PI chains arising from the rigidity of PI molecules, in accordance with the increasing T_gs.

Charge Transfer Interactions

UV/vis transmission spectroscopic measurements were employed to characterize charge transfer (CT) interactions, as shown in Figure 5. The cut-off wavelength is defined as the wavelength at which the transmittance is lower than 1%. The values of cut-off wavelength of BPDA/ODA, BPDA/DABA, BPDA/PDA, BPDA/MABZ, BPDA/BOA, and BPDA/PABZ are 408, 423, 414, 426, 416, and 443 nm, respectively. The values of cut-off wavelength are closely related to the CT interactions and the higher values of cut-off wavelength indicate stronger CT interactions.[32]

BPDA/PABZ and BPDA/BOA PI fibers show similar chemical structure and conformational rigidity. However, cut-off wavelength of the former is much higher than that of the latter. To further research, interactions between molecular chains of BPDA/PABZ and BPDA/BOA PI fibers are selected to be studied by molecular simulation.

For the two kinds of repeat units, the highest occupied molecular orbital (HOMO) is mainly located on PABZ and BOA, whereas the lowest unoccupied molecular orbital (LUMO) is mainly located on BPDA. PABZ and BOA act as electron-donor and BPDA acts as electron-acceptor. As clearly illustrated in Supporting Information Table s2, the calculated HOMO and LUMO energy levels in the ground-state optimized geometry are found to be −5.68 eV and −2.39 eV for BPDA/PABZ and −5.90 eV and −2.40 eV for BPDA/BOA. By comparing the HOMO energy, the increase in the values (−5.68 eV > −5.90 eV) could indicate the stronger electron donating effect and the larger degree of π-conjugation spread between molecules.[33] In contrast, the LUMO energy levels are nearly the same. The increase in HOMO energy level effectively leads to a relatively narrow band gap in BPDA/PABZ (3.29 eV), indicating stronger CT interactions exist between PABZ/BPDA molecular chains.

Mechanical Properties

The mechanical properties of six kinds of PI fibers are tested and shown in Table I. The flexible BPDA/ODA PI fibers show the lowest tensile strength and initial modulus. The tensile strength and modulus of BPDA/BOA PI fibers are higher than that of BPDA/PDA PI fibers, though the rigidity of BPDA/PDA is larger than BPDA/BOA. Therefore, PI fibers with moderate rigid can reach better mechanical properties. When the —O— group in BPDA/ODA is replaced with —CONH— group, the tensile strength of BPDA/DABA PI fibers increases from 0.51 GPa to 0.85 GPa. Obviously, this is due to the strong hydrogen bond interactions between BPDA/DABA molecular chains brought by amide bond.

Table I. Tensile Strength, Initial Modulus, and Elongation of Six Kinds of PI Fibers

Sample	Tensile strength (GPa)	Initial modulus (GPa)	Elongation (%)
BPDA/ODA	0.51	17.7	18.1
BPDA/DABA	0.85	44.7	6.8
BPDA/PDA	1.02	64.1	1.7
BPDA/BOA	1.72	82.4	4.8
BPDA/MABZ	0.74	33.3	12.6
BPDA/PABZ	1.82	85.7	4.2

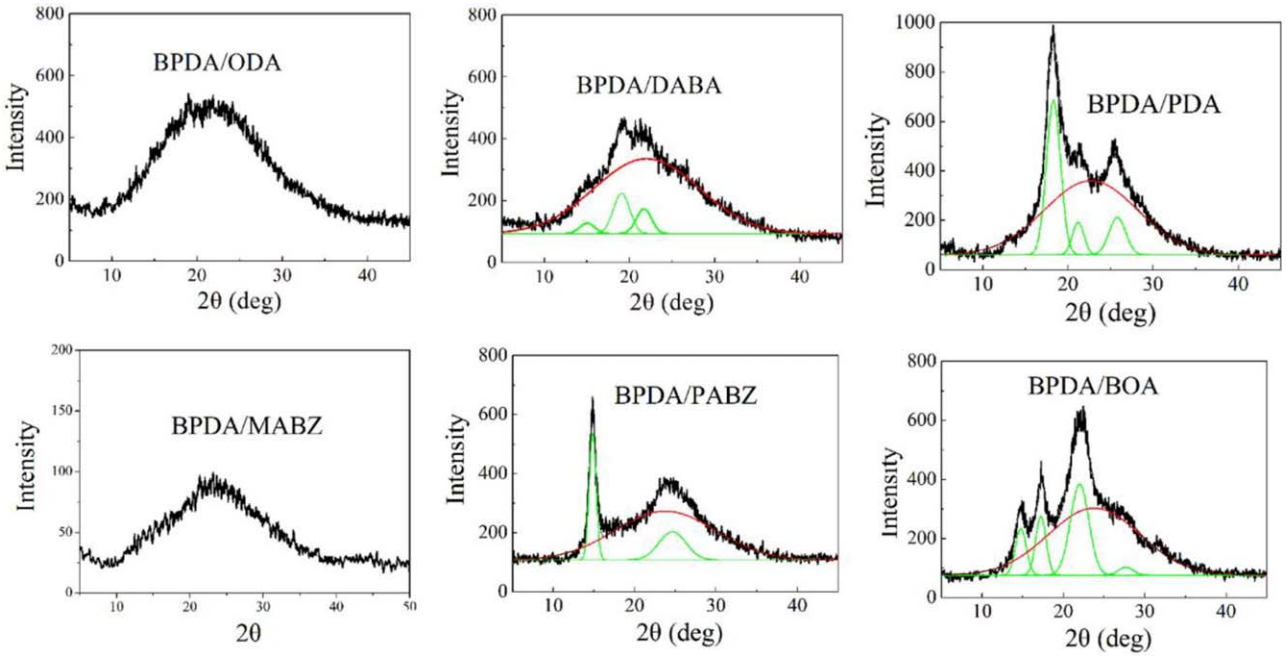

Figure 6. The 1D-WAXD patterns and curve fittings of (a) BPDA/ODA; (b) BPDA/DABA; (c) BPDA/PDA; (d) BPDA/MABZ; (e) BPDA/PABZ; (f)BPDA/BOA PI fibers. [Color figure can be viewed in the online issue, which is available at wileyonlinelibrary.com.]

Similarly, the tensile strength and modulus of BPDA/PABZ PI fibers are higher than BPDA/BOA PI fibers because of the strong hydrogen bond interactions brought by benzimidazole. However, the BPDA/MABZ PI fibers with meta-position benzimidazole groups show lower values of tensile strength and modulus than other kinds of rigid PI fibers (BPDA/PDA, BPDA/BOA, and BPDA/PABZ) though the hydrogen bond interactions between molecular chains are the strongest. Therefore, PI fibers without rigidity cannot reach good mechanical properties though there are strong hydrogen bond interactions. Among six kinds of PI fibers, tensile strength and modulus of BPDA/PABZ are the highest, which can reach 1.81 GPa and 85.7 GPa. Therefore, PI fibers with moderate rigid and strong interactions between molecular chains can reach best mechanical properties.

Performance of Fibers

From the above results and discussion, conformational rigidity and hydrogen bond interactions have an important effect on mechanical properties. Mechanical properties of PI fibers are significantly affected by aggregation structure of macromolecular chains. Therefore, we should further investigate the influence of conformational rigidity and hydrogen bond interactions on aggregation structure. Aggregation structure includes crystallinity and degree of orientation.

1D and 2D WAXD were used to characterize the aggregation structure of six different PI fibers, as shown in Figures 6 and 7. All the diffraction peaks were deconvoluted and fitted with Gaussian broadening functions on a single baseline to estimate the central peak positions. In the equatorial directions from Figure 6, BPDA/PDA, BPDA/BOA, and BPDA/PABZ PI fibers, whose backbones are rigid rod-like, exhibit strong crystalline diffraction peaks. However, BPDA/ODA and BPDA/MABZ PI fibers whose backbones are flexible chain are amorphous. These results are in accordance with the reports that rigid rod-like PI macromolecules tend to pack in order.[34,35]

Crystallization is related to the ordered arrangement of molecular chains, so crystallinity is used to evaluate packing order degree of molecular chains. In 1D-WAXD, crystallinity is calculated with the formula, $X_c = A_c/(A_c + A_a)$.[36] In this formula, X_c is crystallinity; A_c is crystalline peak area; A_a is amorphous peak area. The crystallinities of six different PI fibers are illustrated in Table II. PI fibers with rigid rod-like chains possess higher crystallinities than PI fibers whose backbones are flexible. However, crystallinity of BPDA/PDA PI fibers is 28%, lower than that of BPDA/BOA (32%) PI fibers, though rigidity of BPDA/PDA PI fibers is higher. Therefore, moderate rigidity is beneficial for PI molecular chains to pack in order and crystallize. PI fibers with moderate rigidity show better mechanical properties. Comparing BPDA/PABZ PI fibers with its similar rigidity system (BPDA/BOA PI fibers), we find that the former shows lower crystallinities. It indicates that hydrogen bond interactions will inhibit crystallization.

After curve fitting of 1D-WAXD patterns, every center of peak is located, and interplanar spacing "d" of BPDA/BOA and BPDA/PABZ PI fibers are calculated with Bragg Formula ($2d\sin\theta = \lambda$), as illustrated in Table III.

In the diffraction patterns of BPDA/BOA PI fibers, strong peaks are observed at 14.72°, 17.23°, 21.98°, and 23.79°, while a weak peak appears at 27.67°. Based on indexing analysis of molecular simulations by Zhuang Yongbin, the peak at 14.72° (6.01 Å), which attributes to crystal face (002), is derived from "side to side" stacking.[37] Besides, the interplanar spacing of 6.01 Å is similar to interplanar spacing of copoly(benzobisoxazole) imides

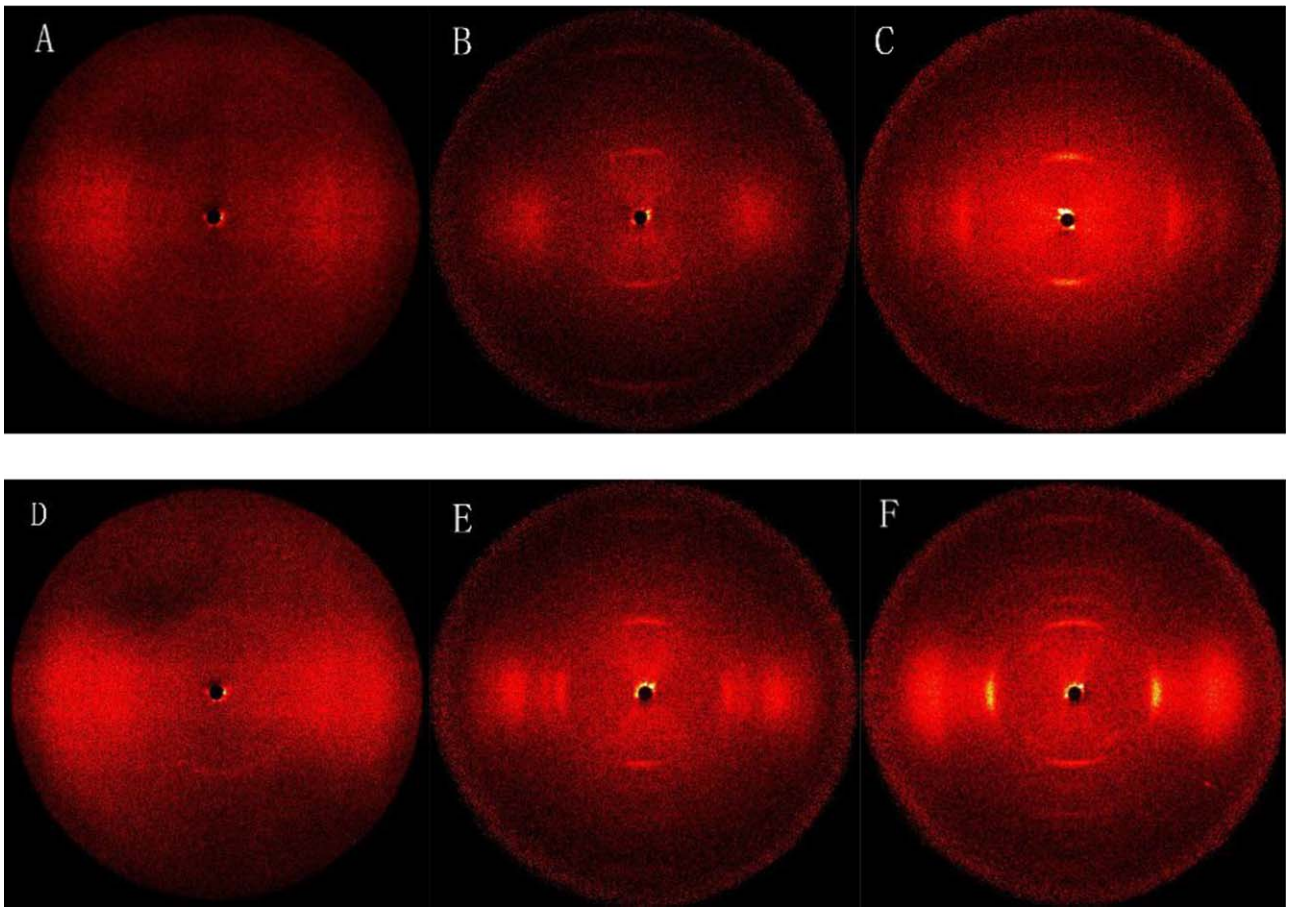

Figure 7. 2D-WAXD patterns of (A) BPDA/ODA; (B) BPDA/DABA; (C) BPDA/PDA; (D) BPDA/MABZ; (E) BPDA/BOA; (F) BPDA/PABZ PI fibers. [Color figure can be viewed in the online issue, which is available at wileyonlinelibrary.com.]

"side to side" stacking.[38] The peak at 21.98° (4.04 Å) is derived from "face to face" stacking of imide ring or benzoxazole ring, and the interplanar spacing of 4.04 Å is similar to interplanar spacing of "π–π" stacking.[35]

In the diffraction patterns of BPDA/PABZ PI fibers, strong peak at 15.01° (5.88 Å) corresponds to "side to side" stacking of BPDA/BOA PI fibers. Li *et al.* demonstrated that interplanar spacing of poly(*p*-phenylene benzobisimidazole) order stacking is 5.5 Å, and the value is close to 5.88 Å,[39] indicating that peak at 15.01° is derived from "side to side" stacking of benzimidazole ring. Besides, peak at 24.63° (3.61 Å) is derived from "π–π" stacking of PI. Both "side to side" stacking and "π–π" stacking interplanar spacings in BPDA/PABZ PI fibers are less than that in BPDA/BOA PI fibers, indicating that hydrogen bond interactions may influence molecular packing and lead to a small interplanar spacing.

In the meridional direction, three diffraction arcs are observed in the 2D-WAXD pattern of BPDA/BOA PI fibers, while two diffraction arcs are observed in the 2D-WAXD pattern of BPDA/PABZ PI fibers. In the 2D-WAXD pattern of BPDA/PABZ PI pattern, diffraction arcs at 14°–15° are lighter than

Table II. Results of Crystallinity, $<\cos^2\psi>_{hkl}$ and f_2 in Crystalline Region of Six Kinds of PI Fibers

Sample	Crystallinity	$<\cos^2\psi>$	f_2
BPDA/ODA	0	0.70	0.55
BPDA/DABA	7	0.79	0.68
BPDA/PDA	28	0.83	0.75
BPDA/BOA	32	0.85	0.77
BPDA/MABZ	0	0.77	0.66
BPDA/PABZ	24	0.86	0.79

Table III. 1D-Wide Angle X-ray Diffraction Position (2θ) and *d*-Spacing in WAXD Patterns of BPDA/BOA and BPDA/PABZ

Sample	2θ (°)	*d* (Å)
BPDA/PABZ	15.01	5.88
	24.63	3.61
	23.76 (amorphous halo)	3.74
BPDA/BOA	14.72	6.01
	17.23	5.14
	21.98	4.04
	27.67	3.22
	23.79 (amorphous halo)	3.74

diffraction arcs at 22°–25°, indicating that "side to side" stacking are more ordered than "π–π" stacking, and the results are in accordance with 1D-WAXD patterns. In both 2D-WAXD patterns of BPDA/BOA and BPDA/PABZ PI fibers, the sixth layer lines in the equatorial direction are the brightest. Besides, their corresponding interplanar spacing are both near 7.2 Å, and the similar values suggest the *c* axis lengths in the unit cells of BPDA/BOA and BPDA/PABZ PI fibers are consistent.

For crystal face (*hkl*), the degree of orientation in crystalline region can be assessed with $<\cos^2\psi>_{hkl}$, which is calculated with the formula[12] $\langle\cos^2\psi\rangle_{hkl}=\frac{\int_0^{\frac{\pi}{2}} I(\psi)\cos x^2\psi\sin\psi d\psi}{\int_0^{\frac{\pi}{2}} I(\psi)\sin\psi d\psi}$. In this formula, ψ represents azimuthal angle, and $I(\psi)$ represents scanning intensity at ψ angle.

In common, f_2 is defined as Herman's orientation function, and determined with Herman Formula $f_2=\frac{3\langle\cos x^2\psi\rangle-1}{2}$.[40] $<\cos^2\psi>_{hkl}$ and f_2 of six PI fibers are shown in Table II.

The rigid rod-like PI fibers (BPDA/PDA, BPDA/BOA, BPDA/PABZ) exhibit higher degree of orientation in crystalline region than the flexible PI (BPDA/ODA, BPDA/MABZ) fibers. Therefore, the rigid rod-like PI fibers possess better mechanical properties. PI fibers with strong hydrogen bond interactions (BPDA/PABZ) possess the highest degree of orientation in crystalline region which is 79%, so strong hydrogen bond interactions can make molecular chains pack more densely and possess higher degree of orientation in crystalline region, and then lead to higher tensile strength and initial modulus.

CONCLUSIONS

Rigidity of molecular chains and hydrogen bond interactions determine aggregation structure by affecting CT interactions, degree of orientation, and crystallization. Aggregation structure finally determines the mechanical properties of PI fibers. Six kinds of PI fibers with different conformational rigidity and interactions are prepared. *D*-values of energy barrier and bottom in potential energy curves of PI units are calculated to measure the rigidity of molecular chains. When *D*-value is less than 28, PI fibers show low conformational rigidity and amorphous structure, leading to poor mechanical properties. When *D*-value increases, PI molecules chains with moderate rigidity tend to pack in order and show better mechanical properties. However, when *D*-value increases to more than 40, the BPDA/PDA PI fibers exhibit high conformational rigidity and crystalline structure. High rigidity leads to difficult molecular chains rotating and fracture mechanisms change from ductile fracture to brittle fracture, which leads to poor mechanical properties. Besides, stronger hydrogen bond interactions can make molecular chains pack more densely and possess higher degree of orientation in crystalline region, and then lead to higher tensile strength and initial modulus. Finally, PI fibers, which possess moderate conformational rigidity and strong hydrogen bond interactions, exhibit highest mechanical properties.

ACKNOWLEDGMENTS

This work was financially supported by the National Natural Science Foundation of China (Grant No. 50973073) and State Key Laboratory of Polymer Materials Engineering (Grant No. sklpme 2014-2-04).

REFERENCES

1. Sroog, C. *Prog. Polym. Sci.* **1991**, *16*, 561.
2. Ghosh, M. Polyimides: Fundamentals and Applications; CRC Press: New York, **1996**.
3. Luo, L.; Zheng, Y.; Huang, J.; Li, K.; Wang, H.; Feng, Y.; Wang, X.; Liu, X. *J. Appl. Polym. Sci.* **2015**, 132, DOI: 10.1002/app.42001.
4. Dong, J.; Yin, C.; Zhang, Z.; Wang, X.; Li, H.; Zhang, Q. *Macromol. Mater. Eng.* **2014**, *299*, 1170.
5. Xia, Q.; Liu, J.; Dong, J.; Yin, C.; Du, Y.; Xu, Q.; Zhang, Q. *J. Appl. Polym. Sci.* **2013**, *129*, 145.
6. Niu, H.; Qi, S.; Han, E.; Tian, G.; Wang, X.; Wu, D. *Mater. Lett.* **2012**, *89*, 63.
7. Hearle, J. W. High-Performance Fibres; Elsevier: Amsterdam, **2001**.
8. Luo, L.; Yao, J.; Wang, X.; Li, K.; Huang, J.; Li, B.; Wang, H.; Liu, X. *Polymer* **2014**, *55*, 4258.
9. Park, S. K.; Farris, R. J. *Polymer* **2001**, *42*, 10087.
10. Gao, G.; Dong, L.; Liu, X.; Ye, G.; Gu, Y. *Polym. Eng. Sci.* **2008**, *48*, 912.
11. Liu, X.; Gao, G.; Dong, L.; Ye, G.; Gu, Y. *Polym. Adv. Technol.* **2009**, *20*, 362.
12. Luo, L.; Pang, Y.; Jiang, X.; Wang, X.; Zhang, P.; Chen, Y.; Peng, C.; Liu, X. *J. Polym. Res.* **2012**, *19*, 9783.
13. Zhang, P.; Chen, Y.; Li, G.; Luo, L.; Pang, Y.; Wang, X.; Peng, C.; Liu, X. *Polym. Adv. Technol.* **2012**, *23*, 1362.
14. Song, G.; Zhang, Y.; Wang, D.; Chen, C.; Zhou, H.; Zhao, X.; Dang, G. *Polymer* **2013**, *54*, 2335.
15. Zhuang, Y.; Gu, Y. *J. Polym. Res.* **2013**, *20*, 1.
16. Li, B.; Pang, Y.; Fan, C.; Gao, J.; Wang, X.; Zhang, C.; Liu, X. *J. Appl. Polym. Sci.* **2014**, *131*, DOI: 10.1002/app.40498.
17. Yin, C.; Dong, J.; Zhang, D.; Lin, J.; Zhang, Q. *Eur. Polym. J.* **2015**, *67*, 88.
18. Lei, X.; Qiao, M.; Tian, L.; Chen, Y.; Zhang, Q. *J. Phys. Chem. C* **2016**, *120*, 2548.
19. Lei, X.; Chen, Y.; Qiao, M.; Tian, L.; Zhang, Q. *J. Mater. Chem.* **2016**, *4*, 2134.
20. Lei, X. F.; Qiao, M. T.; Tian, L. D.; Yao, P.; Ma, Y.; Zhang, H. P.; Zhang, Q. Y. *Corros. Sci.* **2015**, *90*, 223.
21. Lei, X.; Qiao, M.; Tian, L.; Chen, Y.; Zhang, Q. *Corros. Sci.* **2015**, *98*, 560.
22. Lei, X.; Yao, P.; Qiao, M.; Sun, W.; Zhang, H.; Zhang, Q. *High Perform. Polym.* **2014**, *26*, 712.
23. Lei, X. F.; Chen, Y.; Zhang, H. P.; Li, X. J.; Yao, P.; Zhang, Q. Y. *ACS Appl. Mater. Interfaces* **2013**, *5*, 10207.
24. Hu, X. D.; Jenkins, S. E.; Min, B. G.; Polk, M. B.; Kumar, S. *Macromol. Mater. Eng.* **2003**, *288*, 823.

25. Dimitrakopoulos, C. D.; Machlin, E. S.; Kowalczyk, S. P. *Macromolecules* **1996**, *29*, 5818.
26. Zhuang, Y.; Liu, X.; Gu, Y. *Polym. Chem.* **2012**, *3*, 1517.
27. Hegde, M.; Shahid, S.; Norder, B.; Dingemans, T. J.; Nijmeijer, K. *Polymer* **2015**, *81*, 87.
28. Haruki, M.; Hasegawa, Y.; Fukui, N.; Kihara, S. I.; Takishima, S. *J. Appl. Polym. Sci.* **2014**, *131*, DOI: 10.1002/app.39878.
29. Liang, T.; Yang, X.; Zhang, X. *J. Polym. Sci. Part B: Polym. Phys.* **2001**, *39*, 2243.
30. Pan, R.; Liu, X.; Zhang, A.; Gu, Y. *Comput. Mater. Sci.* **2007**, *39*, 887.
31. Rubinstein, M.; Colby, R. H. *Polymer Physics*; OUP Oxford: Oxford, **2003**.
32. Hasegawa, M.; Horie, K. *Prog. Polym. Sci.* **2001**, *26*, 259.
33. Yang, L.; Yu, Y.; Zhang, J.; Song, Y.; Jiang, L.; Gao, F.; Dan, Y. *RSC Adv.* **2014**, *4*, 43538.
34. Takizawa, K.; Wakita, J.; Azami, S.; Ando, S. *Macromolecules* **2010**, *44*, 349.
35. Wakita, J.; Jin, S.; Shin, T. J.; Ree, M.; Ando, S. *Macromolecules* **2010**, *43*, 1930.
36. Wang, N.; Zhang, J.-C.; Sun, R.-J.; Lai, K. *J. Xi'an Univ. Eng. Sci. Technol.* **2007**, *3*, 002.
37. Zhuang, Y.; College of Polymer Science and Engineering, Sichuan University: Chengdu, **2011**.
38. Kolhe, N. B.; Asha, S.; Senanayak, S. P.; Narayan, K. *J. Phys. Chem. B* **2010**, *114*, 16694.
39. Li, S.; Fried, J.; Colebrook, J.; Burkhardt, J. *Polymer* **2010**, *51*, 5640.
40. Sidorovich, A.; Mikhailova, N.; Baklagina, Y. G.; Koton, M.; Gusinkaya, V.; Batrakova, T.; Romashkova, K. *Polym. Sci. USSR* **1979**, *21*, 191.